대한기계학회 2001년도 춘계학술대회논문집 D pp. 232~239 KSME 01S431

MECHANISM OF NUCLEATE BOILING HEAT TRANSFER FROM WIRES IMMERSED IN SATURATED FC-72 AND WATER

전열면적 및 유체의 종류가 핵비등 열전달에 미치는 영향과 그 원인

J. H. Kim*, S. M. You** and J. Y. Pak***

Key Words : Nucleate boiling, Boiling heat transfer mechanism, Latent heat contribution, Micro-convection heat transfer, Consecutive-photo method

Abstract

The present study is an experimental investigation of nucleate boiling heat transfer mechanism in pool boiling from wire heaters immersed in saturated FC-72 coolant and water. The vapor volume flow rate departing from a wire during nucleate boiling was determined by measuring the volume of bubbles, varying 25 μm, 75 μm, and 390 μm, from a wire utilizing the consecutive-photo method. The effects of the wire size on heat transfer mechanism during a nucleate boiling were investigated by measuring vapor volume flow rate and the frequency of bubbles departing from a wire immersed in saturated FC-72. One wire diameter of 390 μm was selected and tested in saturated water to investigate the fluid effect on the nucleate boiling heat transfer mechanism. Results of the study showed that an increase in nucleate boiling heat transfer coefficients with reductions in wire diameter was related to the decreased latent heat contribution. The latent heat contribution of boiling heat transfer for the water test was found to be higher than that of FC-72. The frequency of departing bubbles was correlated as a function of bubble diameters.

1. INTRODUCTION

On a boiling surface, the total heat dissipation can be categorized into four different modes of heat transfer: latent heat, micro-convection, natural convection, and Marangoni flow. Heat transfer associated with latent heat takes place when liquid vaporizes and latent heat dissipates as bubbles leave the heated surface. Micro-convection results from sensible heat energy transferred by entrapment of the superheated liquid in the departing bubble's wake. Natural convection is the sensible energy transport dissipated from non-boiling portions of the heated surface to the surrounding fluid due to density gradients. Marangoni flow is caused by the surface tension gradient while the bubble is still attached onto the surface. For fully developed and saturated nucleate boiling, latent heat transfer and micro-convection are generally considered as primary heat transfer mechanisms because the Marangoni flow effect becomes insignificant when the liquid is saturated and natural convection is negligible when bubbles are fully developed on a heated surface.

In order to establish a fundamental theory of boiling heat transfer mechanism in conjunction with latent heat and micro-convection, the key boiling parameters such as bubble volume flow rate, bubble departure diameter, and bubble departure frequency should be obtained and the relationship among these boiling parameters should be analyzed. The latent heat contribution can be calculated by measuring vapor volume flow rate from a heated surface and micro-convection can be estimated by subtracting the amount of latent heat from a total heat transfer in fully developed and saturated nucleate boiling. The frequency and size of bubbles can be obtained from measuring the bubble volume and counting the number of bubbles departing from a heated surface during a given period. The photographic method is utilized to measure the volume flow rate and bubble sizes.

Many investigators developed numerous photographic methods to investigate boiling parameters and resulting

* Department of Mechanical and Aerospace Engineering, University of Texas at Arlington
** School of Mechanical & Aerospace Engineering, Seoul National University
***BEHR Climate System

data and empirical correlation were broadly utilized to obtain contribution of latent heat to total heat load from a heated surface. In 1933, Jakob and Linke [1] employed high-speed photography to obtain bubble departure diameter and frequency from a single nucleation site and they found the fundamental facts of boiling heat transfer from the experimental results. Rallis and Jawurek [2] were among the first to find the importance of the latent heat contribution during the boiling process. They used bubble frequency and departure diameter measurements from the single nucleation site to calculate vapor flow rates resulted in latent heat contribution. McFadden and Grassmann [3] used high-speed motion pictures to measure departure diameter and frequency of bubbles for pool boiling of liquid nitrogen focusing on observing a relationship between frequency and diameter for the prediction of a frequency spectrum given a bubble diameter spectrum. They also revealed that the existing correlation relating the bubble frequency and diameter was unable to predict their new data. Paul and Abdel-Khalik [4] measured departure bubble diameter, frequency, and active nucleation site density from a wire immersed in saturated water by evaluating approximately 1,000 frames-per-heat flux obtained with a high-speed camera at 6,400 frames-per-second capability. They used 300-μm-diameter platinum wire and found the relation between the latent heat transport by vapor bubbles and experimental data (frequency and diameter of bubbles) from a statistical analysis. Barthau [5] measured departure diameter, frequency, and active nucleation site density using video images of directly reflected light from a heated tube immersed in R-114 coolant at various pressures. Nucleation site density was obtained by scanning a single video image of the heated surface magnified 200 times. Bubble frequency and departure diameter were acquired using successive video images taken in the presence of a stroboscope. Based on his experimental data, Barthau [5] predicted heat transfer per bubble and determined that latent heat played a significant role in the total heat flux. Despite accurate and useful results, the experimental methods listed above require the interpretation of a huge number of individual image frames at every heat flux to quantify the boiling parameters. Due to the difficulty of handling bulk photographic images, many previous investigators were not able to study the wire heater size effect and fluius effect on mechanism of boiling phenomena. In 1998 Ammerman et al. [6] introduced the new photographic technique called "Consecutive-photo method" and the method has been proven to be accurate for measuring volumetric flow rate of bubbles and frequency of bubbles from a boiling surface. The consecutive-photo method also enables comparison study for the mechanism of nucleate boiling heat transfer with various sizes of heated platinum wires in saturated liquid relatively easy since this technique requires relatively few video images to obtain steady-state vapor volume flow rates.

In the present study, the consecutive-photo method is selected to determine the volume flow rate and bubble sizes during nucleate boiling from platinum wires immersed in saturated FC-72. Three platinum wires 25-μm-, 75-μm- and 390-μm-diameter were chosen and investigated in order to understand the wire size effect, based upon You et al. [7].

In addition, the 390-μm-diameter platinum wire was also tested in saturated water and the results were compared with the data of saturated FC-72 to observe fluid effect on nucleate boiling heat transfer. Hong [8] proposed that the wire heater immersed in saturated water would follow the normal behavior of nucleate boiling phenomenon only if the wire size is larger than approximately 300-μm-diameter. Coolant FC-72 is known as a highly wetting dielectric liquid and has relatively poor thermal properties compared to water. Because of their dissimilar properties, a clear insight into the nature of boiling heat transfer mechanism can be made between water and FC-72 by comparing these experimental results.

2. EXPERIMENTAL APPARATUS AND PROCEDURE

2.1 Test Facility

The experimental apparatus for the present study was designed based upon Ammerman et al. [6] and modified for the current research purpose. The figure of the pool boiling test facility is excerpted and modified from Ammerman (1998) and shown in Fig. 1. The test section consisted of an electrically heated platinum wire soldered between two copper terminals that connect the voltage probe and the power supply. The DC power supply was connected to the heater in series with a precision resistor that was used to measure the electrical current to obtain heat flux. The bulk liquid was heated up using six strip heaters attached to the outside of the vessel (four mounted to opposite sides and two to the bottom) and one cartridge heater inside the vessel that accelerates the degassing process. The bottom and sides of the test vessel (except for the lexan windows) were insulated with neoprene to prevent heat loss from the test vessel.

The platinum wire itself was used to measure surface temperature by measuring the resistance since platinum has a uniquely repeatable temperature-versus-resistance relationship. The wire was calibrated prior to experiment to generate the temperature-versus-resistance relationship at various temperatures and confirmed after test to make sure that the wire had not been damaged during the experiment. To minimize Joule heating effect during calibration, the minimum supply voltage (0.03 volts) was applied as suggested by Hong [8].

2.2 Test Procedure

As discussed, the "Consecutive-photo method" introduced by Ammerman et al. [6] was employed to obtain vapor volumetric-flow rate in this study. A high-speed camera captured the images of the domain of interest including bubbles departing from a heated platinum wire during the boiling process. The camera was connected to a personal computer to archive and digitize the images of the bubbles. The camera's frame speed was set to 240 frames per second and the shutter speed was fixed at 1/10,000 of a second. The wire heater was illuminated from the back with a 150-Watts halogen lamp. A sheet of tracing paper was placed on the back of the vessel to diffuse the light from the lamp for accurate measurement of the bubble's size. According to Lunde and Perkins [9], bubbles diameter could be underestimated and inaccurate if a perfect diffuser was used.

Prior to performing the test, electrical power was applied to the cartridge heater and strip heaters to heat up the bulk liquid to its saturation temperature. The test liquid had been kept at saturation conditions for one to two hours while the cartridge heater expedites the degassing process for the removal of non-condensable gases. In order to maintain the atmospheric pressure, the testing vessel was vented to atmosphere. The boiling experiment started after the degassing process, and a heat flux versus wall temperature was generated by incrementing the power supply until CHF was detected. The natural convection region was carefully compared with correlation of Kuehn and Goldstein [10] to verify that the wire calibration method was proper and accurate.

During the boiling test, images of bubbles were taken by the high-speed camera archived as TIF files at four different heat flux data in nucleate boiling regime for all experiments except 390-μm-diameter wire test in saturated water (three heat flux). These increments of heat flux were determined proportionally based on the percentage of CHF to compare each case properly. Using a Global Lab Image computer program, the volumes of bubbles were measured and cumulative average volumetric flow rates were calculated with the "Consecutive-photo method." For the present experiment, a filming rate of 240 frames per second was selected to track the individual bubbles from frame to frame. Each series of photographs was evaluated, four frames at a time, to count and measure the size of individual bubbles. In each frame, a reference line was placed parallel to the wire at given height as a reference location for counting bubbles passing the line at a given time. The total of the individual bubble volume was calculated and divided by the time interval between the first frame and fourth frame. This instantaneous vapor volume flow rate was repeated for all series sets until the cumulative volume flow rate becomes steady-state. Also, the bubble frequency per unit area of a wire was measured to investigate the mechanism of nucleate boiling heat transfer from a wire heater immersed in saturated liquid.

2.3 Experimental Uncertainty

Uncertainties in nucleate boiling volume flow rate measurements and latent heat calculation for 75-μm-diameter platinum wire in saturated FC-72 are performed. This uncertainty analysis was done as same manner with Ammerman et al. [6] since the setting and procedure of experiment was identical. The uncertainties in vapor volumetric flow rate and latent heat flux for the present study were estimated to be no more than ±8.3% and ±9.3% respectively. Both vapor volumetric flow rate and Latent heat flux uncertainties for a 95% confidence level were calculated using the method of Kline and McClintock [11].

3. RESULTS AND DISCUSSION

The present study is to understand the mechanism of nucleate boiling heat transfer from wires as varying wire size and working fluids. The boiling curves were obtained in the form of wall temperature versus heat flux for each case. Natural convection data were compared with the natural convection correlation of Kuehn and Goldstein [10] for the qualification of the present data. Fig. 2 shows this comparison and the excellent agreement was made between the experimental data and the correlation. The boiling parameters (volumetric flow rate, departure diameter and frequency of bubbles) were obtained for each case to investigate the mechanism of nucleate boiling heat transfer.

3.1 Size Effect of Platinum Wires Immersed in Saturated FC-72

25-μm, -75-μm and 390-μm-diameter platinum wires were tested and compared one to another to investigate the size-effect on mechanism of nucleate boiling heat transfer. The boiling curves were plotted for these three wires to compare the size-effect of wire in Fig. 3(a). The heat transfer coefficient remains approximately same at low heat flux (discrete bubble region) and the nucleate boiling enhancement begins to occur at fully developed nucleate boiling region as the wire size decreases in Fig. 3(a). These results imply that the isolated bubbles at low heat flux seem to transfer the heat from wires to ambient fluid at approximately same rate regardless of the wire size. However, the enhancement of boiling heat transfer by reducing wire sizes was obviously detected at high heat flux region and this phenomenon shows the wire size effect on nucleate boiling heat transfer.

The sample images of bubbles for 25-μm-, 75-μm-, and 390-μm-diameter wire are shown in Fig. 4(a), (b), and (c) respectively. In the present study, the images of bubbles were achieved at four different heat fluxes (11.6×10^4, 16.3×10^4, 21.4×10^4, 24.1×10^4 W/m^2) for 25-μm-diameter wire, the images of bubbles were achieved also at four different heat fluxes (7.1×10^4, 11.1×10^4, 14.4×10^4, 17.7×10^4 W/m^2) for 75-μm-diameter wire, and the images of bubbles were captured at four different heat fluxes (6.0×10^4, 10.5×10^4, 13.1×10^4, 16.0×10^4 W/m^2) for 390-μm-diameter wire. From the consecutive photo images, majority of the bubbles seem to merge with neighboring bubbles prior to or right after departure at all heat fluxes. Therefore, the bubble diameters and frequencies measured in the present study represent secondary or tertiary bubbles rather than actual departure diameter from a single nucleation site. This observation of bubble merging means that all fluxes investigated in the present study are practically in the regime of mutual bubble interaction.

By using image processing program, a cumulative volume flow rate was acquired at each heat flux and is presented versus measurement time. Due to relatively high fluctuation of cumulative volume flow rate for heat fluxes of 16.0×10^4 W/m^2 on 390-μm-diameter wire, the total duration of measurement time for frames was extended to 0.25 seconds for greater accuracy. Fig. 5 shows the graphs of cumulative time average vapor volume flow rate for each of the four heat fluxes examined in 75-μm-diameter wire in saturated FC-72. The values of volume flow rates are shown as steady-state about after 0.15 seconds except the highest heat flux point of 390-μm-diameter wire. Approximately after 0.2 seconds, the volume flow rate is quite stabilized at the highest heat flux point of 390-μm-diameter platinum wire.

The process of liquid heating, nucleation, growth of bubble, and departure can be referred to the main mechanism of heat transfer during nucleate boiling. In this experiment, the steady-state vapor volume flow rates measured with the consecutive-photo method were used for estimating the latent heat portion to the total heat transfer from the heated wire. The following equation was used to compute latent heat flux:

$$q_{lat} = \frac{\rho_g \dot{V}_g h_{fg}}{\pi DL} \qquad (1)$$

where ρ_g is the vapor density, h_{fg} is the latent heat of vaporization, and D stands for diameter of platinum wire and L is length of wire examined. In Equation (1), volume flow rate is only variable factor to determine the function of latent heat since the density and heat of vaporization are assumed as constant over the test. Comparison plots of latent heat flux versus total heat flux applied for these experiments are shown in Fig. 6. From Fig. 6, the latent heat contribution increases, as the size of wire increases. This trend implies that micro-convection contribution increases while the latent heat portion decreases as the wire size decreases under the assumption of negligible natural convection and Marangoni flow effect. Therefore, increasing the portion of micro-convection within total heat flux provides the enhancement of nucleate boiling heat transfer coefficient. In other words, the micro-convection plays an important role in enhancement of boiling heat transfer when the size of wire reduces.

In order to compare the size and frequency of bubbles rising from the wires, the plot of average diameter and average frequency per unit area of bubbles while increasing the heat flux is shown for each wire in Fig. 7 and Fig. 8, respectively. The figures show that departure diameter decreases and bubble frequency per unit wire area increases as the wire size decreases. These trends combined to result in a decrease in the latent heat transfer contribution and also an increase in the micro-convection contribution for the smaller size wire as observed in Fig. 6. The bubble departure takes place when the size of the bubble becomes so large that it is not possible to maintain a buoyant force-surface tension force balance on the bubble. As the diameter of bubble increases, the surface tension force between the bubble and wire, keeping bubbles from departing due to the buoyant force, increases relatively slower than the buoyant force. The perimeter of contact surface between bubble and wire surface increases linearly to the bubble diameter increase. On the other hand, the increase of buoyant force for the same bubble size increase occurs in proportion to the 3rd power of the bubble diameter. Therefore, at a critical bubble radius, the bubble departs from the heated surface. Since the perimeter of contact surface between the bubble and wire decreases as the wire size decreases, the buoyant force required detaching the bubbles for smaller size of wire relatively decreases compared to larger size of wire. Consequently the bubble departure occurs with smaller volume of bubbles (smaller buoyant force) when the wire size decreases and this phenomenon provides the higher bubble frequency due to the reduced bubble growth time. This higher frequency with smaller bubbles increases the heat transfer rate in boiling heat transfer since the more frequent bubble departure induces thinner superheated liquid layer along the wire. As heat flux is increased in Figs. 7 and 8, the average diameter of bubbles tends to increase for each wire whereas the average frequency per unit area stays fairly constant. Moreover, at the heat flux value of 16.0×10^4 W/m^2 for 390-μm-diameter wire, the average diameter increases much more rapidly and the frequency of bubbles shows a significant decrease. In general, more bubbles appeared to merge and grow together before departure from the wire for the 390-μm-diameter case and the merging became more serious at the high heat flux value.

Frequency distributions over the diameter of bubbles are shown in Fig. 9 in order to investigate the formation of bubbles at different heat flux. Fig. 9 shows that the distribution range of diameter for 75-μm-diameter wire is narrower than that of 390-μm-diameter wire. Furthermore, it is shown that 75-μm-diameter wire produces smaller bubbles with higher bubble frequency than 390-μm-diameter wire, and at 16.0×10^4 W/m^2 significant bubble merging occurred with 390-μm-diameter wire case. These observations confirmed that increasing micro-convection is a dominating factor for enhancement of boiling heat transfer for size effect.

3.2 Fluid Effects on Nucleate Boiling Phenomenon

A 390-μm-diameter platinum wire was tested in saturated water to observe the effects of working fluid on the nucleate boiling heat transfer. The boiling curves for both FC-72 and water are plotted and shown in Fig. 3(b). In Fig. 3(b) the heat transfer coefficient for water is higher than FC-72 for entire range of heat flux. Also, the heat transfer coefficient for water increases more rapidly than FC-72 with increasing heat flux. The images of bubbles were recorded at four different heat fluxes (39×10^4, 50×10^4, 60×10^4, 70×10^4 W/m^2) for same 390-μm-diameter wire for comparison purpose. The sample pictures of bubbles for 390-μm are shown in Fig. 4(d) and (e) along with the images in saturated FC-72. Since numerous bubbles are overlapped and touched one another as shown in Fig. 4(d), the heat flux of 39×10^4 W/m^2 for 390-μm-diameter platinum wire was excluded inevitably while reducing the data in order to maintain the measurement accuracy of this study. A cumulative volume flow rate was acquired at each heat flux. For 390-μm-diameter platinum wire in saturated water, the total duration of measurement time for every heat flux was 0.19 seconds since the cumulative volume flow rates were settled down as steady-state within 0.15 seconds.

The latent heat flux in saturated water was calculated using Equation (1) and plotted with 390-μm-diameter FC-72 data to quantify its contribution to total heat flux in Fig. 10. The latent heat portion during the nucleate boiling in saturated water is larger than that of saturated FC-72 case for the same 390-μm-diameter wire. Therefore, it is inferred that the latent heat contribution is a major factor for the higher boiling heat transfer efficiency in saturated water since the heat of vaporization of water is comparatively large. While the specific heat of water is higher than FC-72 by approximately 400%, the heat of vaporization for water is much larger than FC-72 by 2,400%.

To observe the bubble frequency distribution of diameter of individual bubbles in saturated water, the plot of bubble frequency per unit area versus diameter of bubbles is shown in Fig. 11. Dissimilarly with FC-72, all data points regardless of heat flux show a similar trend. The figure clearly shows that the diameter of bubbles is reduced with the frequency increase of departing bubbles. It was previously observed by Jakob [12] that the bubbles leave a given nucleation site at roughly equal time intervals, and further that the bubbles from this site are approximately of equal diameter. Jakob [12] presented some experimental data and mentioned that over a range of diameters the data could be approximated by the expression:

$$f \cdot D = \text{constant} \qquad (2)$$

where f is the frequency with which the bubbles leave a given site and D is the diameter of these bubbles at the instant they leave the surface. Fig. 11 also shows the trend line of the current data, and the correlation of this trend line is expressed as following:

$$f \cdot D^{4.85} = 7.2 \times 10^{-8} \qquad (3)$$

where f is frequency of bubbles per unit area and D is diameter of departing bubble.

4. CONCLUSIONS

The mechanism of pool boiling heat transfer from a wire immersed in saturated FC-72 and water was investigated using 25-μm, 75-μm and 370-μm-diameter platinum wires. The experimental results were observed and converted into useful data set to understand the nucleate boiling phenomena. All tests were performed at atmospheric pressure under increasing heat flux. The images of bubbles were captured and shown to reveal the factors of boiling enhancement.

1) For a wire immersed in saturated FC-72 under fully developed nucleate boiling regime, a reduction in heater diameter scale provides enhancement of nucleate boiling heat transfer due to the relatively reduced surface tension. This resulted in smaller bubbles departing with higher frequency producing more contribution from micro-convection heat transfer and less contribution from latent heat transfer.
2) The bubble departure diameter decreases and departure frequency increases as length scale is reduced. The distribution range of departure diameter for 75-μm-diameter wire is much narrower than for 390-μm-diameter wire.
3) Even though the larger bubbles with lower bubble frequency were measured in saturated water than in saturated FC-72, the boiling heat transfer rate of saturated water is higher than that of saturated FC-72. Consequently, the latent heat contribution for water is larger than FC-72. This was attributed to the fact that the heat of vaporization for saturated is approximately 24 times higher than FC-72 while the specific heat for saturated water is only four times larger than saturated FC-72. Other fluids should be tested to better understand the effect of different fluids on boiling heat transfer mechanism.
4) Regardless of heat flux values, the formation behavior (size and frequency of bubbles) of bubbles while increasing heat flux appears to be identical in water. This trend was captured as;

$$f \cdot D^{4.85} = 7.2 \times 10^{-8}$$

REFERENCES

(1) Jakob, M., and Linke, W., 1933, "Der Warmeubergang von einer waagerechten Platte an siedendes Wasser," Forsch. Geb. Ing., Vol. 4, p. 75

(2) Rallis, C.J., and Jawurek, H.H., 1964, "Latent Heat Transport in Saturated Nucleate Boiling", Int. J. Heat Mass Transfer, Vol. 7, pp. 1051-1068.

(3) McFadden, P.W. and Grassmann, P., 1962, "The Relation Between Bubble Frequency and Diameter During Nucleate Pool Boiling," International Journal of Heat and Mass Transfer, Vol. 5, pp. 169-173.

(4) Paul, D.D., and Abdel-Khalik, S.I., 1983, "A Statistical Analysis of Saturated Nucleate Boiling Along a Heated Wire," International Journal of Heat and Mass Transfer, Vol. 26, pp. 509-519.

(5) Barthau, G., 1992, "Active Nucleation Site Density and Pool Boiling Heat Transfer-An Experimental Study," International Journal of Heat and Mass Transfer, Vol. 35, pp. 271-278

(6) Ammerman, C.N., and You, S.M., 1998, "Consecutive-Photo Method to Measure Vapor Volume Flow Rate During Boiling From a Wire Immersed in Saturated Liquid," ASME Journal of Heat Transfer, Vol. 120, pp. 561-567.

(7) You, S.M., Hong, Y.S. and O'Connor, "The Onset of Film Boiling on Small Cylinders: Local Dryout and Hydrodynamic Critical Heat Flux Mechanism," Int. J. Heat Mass Transfer, Vol. 37, pp. 2561-2569.

(8) Hong, Y. S., 1992, Critical Heat Flux Mechanism on Small Cylinders, Masters Thesis, The University of Texas at Arlington, TX.

(9) Lunde, K. and Perkins, R.J., 1995, "A Method for the Detailed study of Bubble Motion and Deformation," Proceedings of the 2nd International Conference on Multiphase Flow, Kyoto, pp. 395-405.

(10) Kuehn, T.H. and Goldstein, R. J., 1976, "Correlating Equations for Natural Convection Heat Transfer between Horizontal Circular Cylinders," Int. J. Heat Mass Transfer, Vol. 19, pp. 1127-1134.

(11) Kline, S.J., and McClintock, F.A., 1953, "Describing Uncertainties in Single-Sample Experiments," Mechanical Engineering, Vol. 75, No. 1, pp. 3-8.

(12) Jacob, M., 1958, "Heat Transfer, Vol. 1," John Wiley, New York.

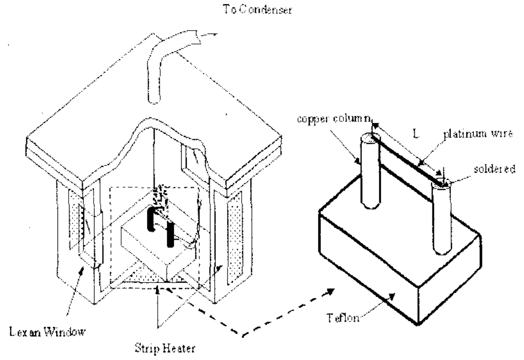

Fig. 1. Pool boiling test facility.
(Excerpted and modified from Ammerman (1998))

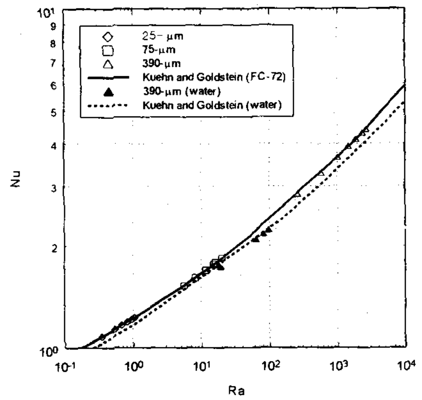

Fig. 2. Natural convection data (FC-72 and water).

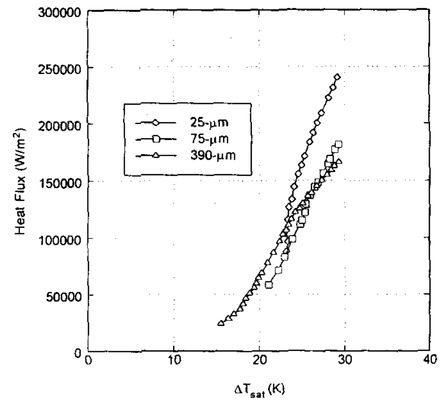

3-(*a*)

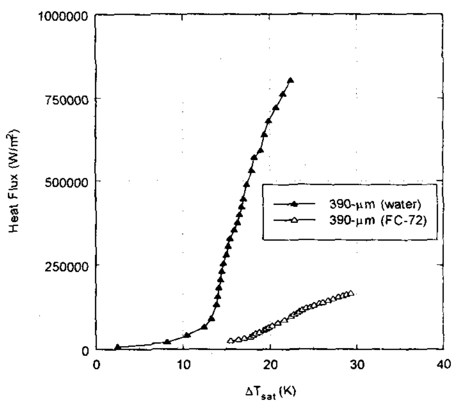

3-(*b*)

Fig. 3. Pool boiling curves (*a*) wire size and (*b*) working fluids effect

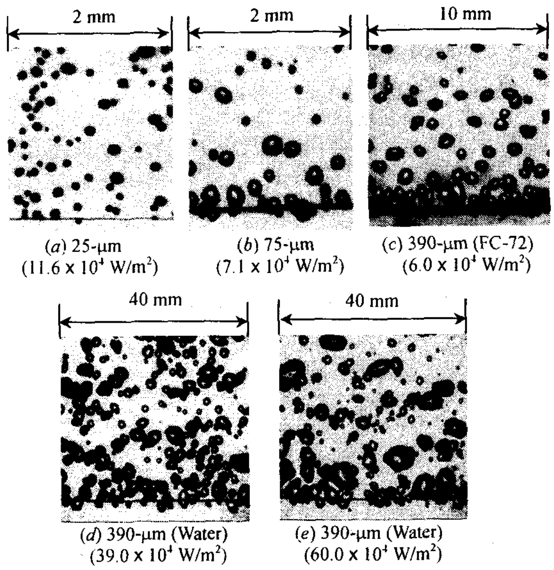

Fig. 4. Sample pictures of bubbles

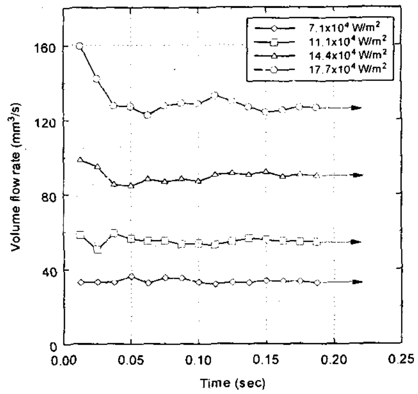

Fig. 5. Cumulative volume flow rate vs time for 75-µm-diameter wire immersed in saturated FC-72

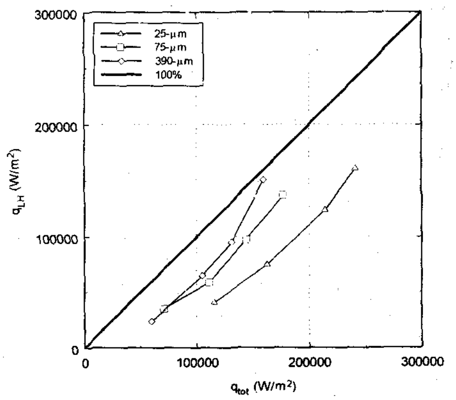

Fig. 6. Latent heat versus total heat flux (wire size effect)

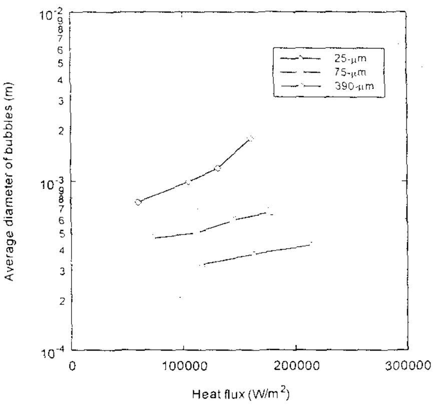

Fig. 7. Average diameter of bubbles departing from wires (increasing heat flux)

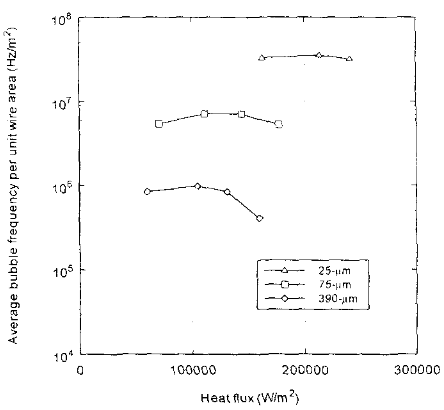

Fig. 8. Average bubble frequency per unit wire area (increasing heat flux)

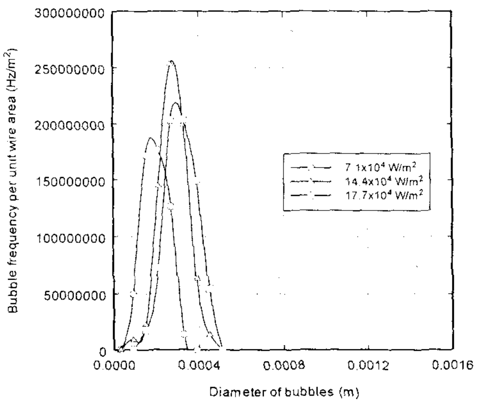

9-(*a*)

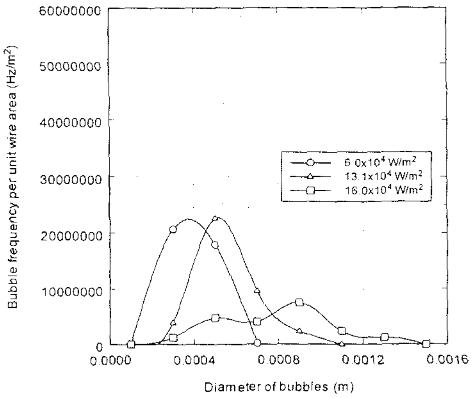

9-(*b*)

Fig 9. Bubble frequency distribution of diameter of bubbles (*a*) 75-μm and (*b*) 390-μm

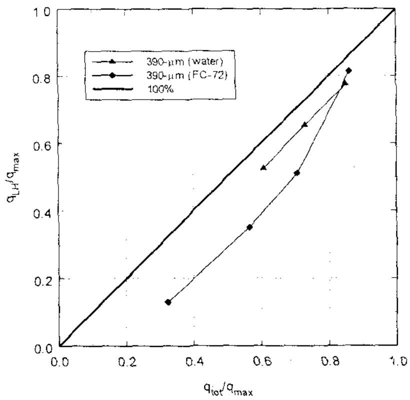

Fig. 10. Latent heat flux versus total heat flux (fluid effect)

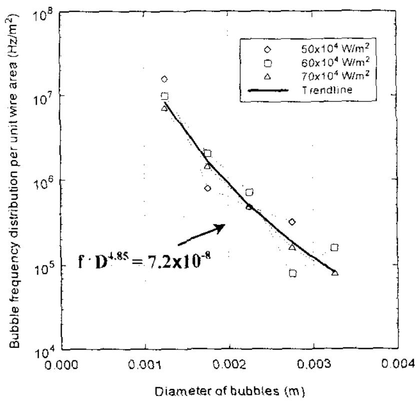

Fig. 11. The trend line of frequency per unit wire area versus diameter of bubbles for 390-μm-diamter wire in saturated water.